A ω-circulant regularization for linear systems arising in interpolation with subdivision schemes

R. Diaz Fuentes, M. Mazza, S. Serra-Capizzano

Abstract

In the curve interpolation with primal and dual form of stationary subdivision schemes, the computation of the relevant parameters amounts in solving special banded circulant linear systems, whose coefficients are related to quantities arising from the used stationary subdivision schemes. In some important cases it happens that the associated generating function, which is a special Laurent polynomial called symbol, has zeros on the unit complex circle of the form $\exp(2\pi \mathrm{i} j/n)$, where n is the size of the matrix, $\mathrm{i}^2 = -1$, and j is a non-negative integer bounded by $n-1$. When this situation occurs the discrete problem is ill-posed simply because the circulant coefficient matrix is singular and the problem has no solution (or infinitely many). Standard and nonstandard regularization techniques such as least square solutions or Tikhonov regularization have been tried, but the quality of the solution is not good enough. In this work we propose a structure preserving regularization in which the circulant matrix is replaced by the ω-circulant counterpart, with ω being a complex parameter. A careful choice of ω close to 1 (recall that the set of 1-circulants coincides with standard circulant matrices) allows to solve satisfactorily the problem of the ill-posedness, even if the quality of the reconstruction is reasonable only in a restricted number of cases. Numerical experiments and further algorithmic proposals are presented and critically discussed.

1 Introduction

When dealing with curve interpolation problems by means of primal and dual form of stationary subdivision schemes [11, 18], the computation of the relevant parameters asks for the solution of certain banded circulant linear systems. The entries of such matrices are related to quantities arising from the adopted stationary subdivision scheme. The associated generating function, a special Laurent polynomial called symbol, in some important cases shows zeros on the unit complex circle of the form $\exp(2\pi \mathrm{i} j/n)$, where n is the size of the matrix, $\mathrm{i}^2 = -1$, and j is a non-negative integer at most equal to $n-1$. In such cases, the discrete problem is ill-posed because of the singular character of the circulant coefficient matrix and the problem does not admit solution or it has infinitely many ones. As is typical in the treatment of ill-posed problems, regularization techniques like least square solutions [14] or Tikhonov regularization can be applied, but the quality of the provided solution is not acceptable.

Our proposal consists in a structure preserving regularization obtained replacing the circulant matrix with its ω-circulant counterpart, where ω is a complex parameter close to 1. Such choice of ω is driven by the fact that the set of 1-circulants coincides with standard circulant matrices. The resulting method allows to satisfactorily solve the problem of the ill-posedness and in some special cases brings to interpolating solutions. More precisely, we take into account the following facts and observations.

A) ω-circulant matrices with any choice of the complex parameter ω show the same computational power and advantages of the standard circulants; in fact the ω-circulant matrices form an algebra simultaneously diagonalized by the matrix $F_{n,\omega}$, where the latter can be written as a diagonal matrix times the Fourier matrix F_n.

B) Even if the computational cost of any operation (computation of eigenvalues, inversion, solution of linear systems, matrix-vector and matrix-matrix product) is equivalent to that arising in the circulant case, i.e., that of few fast Fourier transforms, the numerical stability is dictated (almost) quadratically by the modulus of the parameter r with $r = \max\{|\omega|, |\omega|^{-1}\}$. Indeed, due to expression of $F_{n,\omega}$ and owing to the unitary character of the Fourier matrix F_n, we deduce that the spectral condition number of $F_{n,\omega}$ is exactly $r^{\frac{2(n-1)}{n}}$ and hence the transform matrix $F_{n,\omega}$ is perfectly conditioned (minimal spectral condition number equal to 1) if and only if $|\omega| = 1$. Therefore, for combining a fast method with the most stable computation, we choose our regularization parameter ω as $\omega \neq 1$ and $|\omega| = 1$.

C) Since the regularization process has to produce a perturbed mathematical problem close enough to the original ill-posed one, we set $\omega = \exp(\mathrm{i}\psi)$ with ψ real and small in modulus such that the new coefficient matrix A_ω is close to the original circulant coefficient matrix A and it is invertible: we notice that due to the computational features of the ω-circulants simple tests of invertibility are available with complexity of $O(n \log n)$ arithmetic operations and with a moderate constant hidden in the big $O(\cdot)$.

D) Since the regularized solution is not real, simply because A_ω is not real, and since we need a real solution, with regard to the choice reported in Item C), we take the real part of the solution. Indeed ω is close to 1 and consequently the imaginary part of the solution is small enough and this represents the reason why the proposed approximation makes sense.

The ω-circulant regularized solution sketched in Items A), B), C), D) satisfactorily faces the ill-posedness of the problem as emphasized in the numerical section. Furthermore, the approach is quite flexible and in fact it can be adapted to the block case using ω-block-circulants, so allowing the treatment of more general subdivision problems, e.g., in Hermite form. However, from a model viewpoint, the practical solutions are not always good enough and further work is needed.

The paper is organized in the following manner. In Section 2 we first provide a brief description of the problem, we introduce notations and tools, and then we report the analysis of our procedure. Section 3 contains few selected numerical experiments and relevant comments on the quality of our practical results, while Section 4 is devoted to conclusions and to discuss open problems.

2 Main result

A subdivision scheme is an iterative method that generates curves and surfaces based on successive refinements of a polygon or a mesh. The rules for the refinements can be formulated by linear, non-linear or geometrical operators [12, 11, 8, 18, 2]. The case of linear rules has a relation with the refinable functions in Wavelets Theory [4]. In this setting, the vertices of the polygon or mesh are the coefficients in a particular basis of the so called *subdivision curve* or *subdivision surface*. In what follows we focus on the curve case.

Linear uniform subdivision schemes are related to *refinable functions* $\varphi(t)$ satisfying a relation of the form

$$\varphi(t) = \sum_{j\in\mathbb{Z}} a_j \varphi(2t-j), \quad t \in \mathbb{R}, a_j \in \mathbb{R}, \tag{1}$$

such that given an initial set of *control points* $\mathbf{P}^0 = \{P_j^0 \in \mathbb{R}^m, j = 0,\dots,n-1\}$, the closed curve (considering the periodization $P_j^0 = P_{j+n}^0, j \in \mathbb{Z}$)

$$c(t) = \sum_{j=0}^{n-1} P_j^0 \varphi(t-j), \qquad t \in \mathbb{R} \tag{2}$$

can be also represented as

$$c(t) = \sum_{j=0}^{2^k n-1} P_j^k \varphi\left(2^k t - j\right), \qquad t \in \mathbb{R}$$

where

$$P_i^{k+1} = \sum_{j=0}^{2^k n-1} a_{i-2j} P_j^k, \qquad k \in \mathbb{N},\ i = 0,\dots,2^{k+1}n-1. \tag{3}$$

The relation in (3) is known as *subdivision rule* that defines a *subdivision scheme* and the coefficients in (1) form the so-called *subdivision mask* $\mathbf{a} = \{a_j, j \in \mathbb{Z}\}$. Then, a subdivision scheme is an iterative method where a curve is generated by repeated refinements of an initial polygon. In order to check convergence of the scheme, it is proved that the sequence of polygons with vertices in $\mathbf{P}^k$ converges uniformly to a smooth curve $c(t)$. In practice, just a few amount of iterations are enough to provide a polygon that looks smooth for the human eye.

The sampling of the curve at integer parameters can be found from (1) in the following way

$$c(s) = \sum_{j=0}^{n-1} P_j^0 \varphi\left(s-j\right), \qquad t \in \mathbb{Z}, s \in \mathbb{Z}. \tag{4}$$

The values of $\varphi(\mathbb{Z})$ provide the so called *first limit stencil* $\boldsymbol{\beta}^0 = \left\{\beta_j^0 = \varphi(j),\ j \in \mathbb{Z}\right\}$ and can be computed from a linear system of equations derived from (1) [19] or by spectral analysis of the *local subdivision matrix* [18, 10, 6]. The *second limit stencil* and higher order stencils $\boldsymbol{\beta}^{k-1} = \left\{\beta_j^{k-1} = \varphi^{(k-1)}(j),\ j \in \mathbb{Z}\right\}$, $k \in \mathbb{N}$, $k \geq 1$ can be similarly computed. Thus, by (2) it holds that the k-th derivative of the curve at dyadic parameters $t = \mathbb{Z}/2^m$ can be computed as

$$c^{(k)}\left(\tfrac{s}{2^m}\right) = \sum_{j=0}^{n-1} \beta_{s-j}^k P_j^m. \tag{5}$$

The mask and the stencils have a compact support, defining that way in (1) a basic function of compact support. Therefore we are dealing with finite masks and stencils and although we use the integer indices, just a finite number of them corresponds to non-zero elements.

Let us consider the interpolation of n points $\mathbf{V}^0 = \{V_j^0 \in \mathbb{R}^m, j = 0, \ldots, n-1\}$ with a subdivision curve. The natural idea is to think that those points are a sampling of the curve at integer parameters $V_s^0 = c(s)$, $s = 0, \ldots, n-1$, like in (4), and this leads to the linear algebra problem:

$$M_n \mathbf{P}^0 = \begin{bmatrix} \beta_0 & \beta_{-1} & \beta_{-2} & \ldots & \beta_2 & \beta_1 \\ \beta_1 & \beta_0 & \beta_{-1} & \ldots & \beta_3 & \beta_2 \\ \ddots & \ddots & \ddots & \ddots & \ddots & \ddots \\ \beta_{-1} & \beta_{-2} & \beta_{-3} & \ldots & \beta_1 & \beta_0 \end{bmatrix} \begin{bmatrix} P_0^0 \\ P_1^0 \\ \vdots \\ P_{n-1}^0 \end{bmatrix} = \begin{bmatrix} V_0^0 \\ V_1^0 \\ \vdots \\ V_{n-1}^0 \end{bmatrix} = \begin{bmatrix} c(0) \\ c(1) \\ \vdots \\ c(n-1) \end{bmatrix}. \tag{6}$$

We refer to M_n as the matrix that represents the *point interpolation operator* for linear subdivision schemes. The first row of the matrix M_n is the vector:

$$\boldsymbol{\beta}_n := [\beta_0, \beta_{-1}, \ldots, \beta_{-p}, 0, \ldots, 0, \beta_q, \ldots, \beta_1] \in \mathbb{R}^m,$$

with indices of β_k ranging from $-p$ to q. The structure of that matrix is therefore circulant (see Definition 2.2 below), with some particular cases to be analyzed dependently on the symmetry of the stencils.

Definition 2.1. *A subdivision scheme is said to be* odd-symmetric *if* $a_{-j} = a_j$ *and* even-symmetric *if* $a_{1-i} = a_i$ *for* $j \in \mathbb{N}$.

These symmetries are particular cases of the primal [17] and dual [9] form of subdivision schemes respectively, and the limit stencils have the same kind of symmetries [18].

It follows that the odd-order limit stencil inherits the odd or even symmetry:

$$\beta_j^{2d} = \begin{cases} \beta_{-j}^{2d}, & \text{for odd-symmetric schemes} \\ \beta_{1-j}^{2d}, & \text{for even-symmetric schemes} \end{cases}, \qquad d \in \mathbb{N}.$$

For the even-order limit stencil then we get:

$$\beta_j^{2d+1} = \begin{cases} -\beta_{-j}^{2d+1}, & \text{for odd-symmetric schemes} \\ -\beta_{1-j}^{2d+1}, & \text{for even-symmetric schemes} \end{cases}, \qquad d \in \mathbb{N}. \tag{7}$$

For $d \geq 1$ we have $\displaystyle\sum_{j \in \mathbb{Z}} \beta_j^d = 0$ and $\displaystyle\sum_{j \in \mathbb{Z}} \beta_j^0 = 1$.

2.1 The block-circulant case for Hermite interpolation

In case of interpolating points and associated derivatives up to the $(d-1)$-th order, with tangent interpolation as the first case, the equation (5) provides us a first insight. Let $\mathbf{U}^{(d)} = [V_0^0, V_0^1, \ldots, V_0^{d-1}, V_1^0, V_1^1, \ldots, V_1^{d-1}, \ldots, V_{n-1}^0, V_{n-1}^1, \ldots, V_{n-1}^{d-1}]^T$ be the data that we want to interpolate. We can suppose that there exists a parameter sequence $\{t_j, j = 0, \ldots, n-1\}$ such that the subdivision curve $c(t)$ interpolates the data information in $\mathbf{U}^{(d)}$, i.e.,

$$c^{(k)}(t_j) = V_j^k, \qquad \text{for } k = 0, \ldots, d-1, \; j = 0, \ldots, n. \tag{8}$$

If the curve $c(t)$ is defined by n control points like in (6), then we get solution for the point interpolation problem (6) that may contradicts the values of higher order derivatives.

Thus, in order to interpolate all the information in $\mathbf{U}^{(d)}$, we need to use nd control points $\mathbf{P}^0 = \{P_j^0 \in \mathbb{R}^m, j = 0, \dots, nd-1\}$. A natural choice is to consider the parameters in (8) to be $t_j = dj$, $j = 0, \dots, n-1$. Then, from (5) we get the nd equations:

$$c^{(k)}(dj) = V_{dj}^l = \sum_{s=0}^{n-1} P_j^0 \beta_{dj-s}^l, \qquad j = 0, \dots, n-1,\ k = 0, \dots, d-1. \tag{9}$$

These equations can be represented in a matrix form as:

$$\mathbf{M}_n \mathbf{P}^0 = \begin{bmatrix} \boldsymbol{B}_0 & \boldsymbol{B}_{-1} & \boldsymbol{B}_{-2} & \dots & \boldsymbol{B}_2 & \boldsymbol{B}_1 \\ \boldsymbol{B}_1 & \boldsymbol{B}_0 & \boldsymbol{B}_{-1} & \dots & \boldsymbol{B}_3 & \boldsymbol{B}_2 \\ \ddots & \ddots & \ddots & \ddots & \ddots & \ddots \\ \boldsymbol{B}_{-1} & \boldsymbol{B}_{-2} & \boldsymbol{B}_{-3} & \dots & \boldsymbol{B}_1 & \boldsymbol{B}_0 \end{bmatrix} \begin{bmatrix} P_0^0 \\ P_1^0 \\ \vdots \\ P_{nd-1}^0 \end{bmatrix} = \mathbf{U}^{(d)}, \tag{10}$$

where the $d \times d$ blocks of the matrix $\mathbf{M}_n \in \mathbb{R}^{nd \times nd}$ satisfy $\boldsymbol{B}_j = \boldsymbol{B}_{j-n}$ for $j = 1, \dots, n$ and

$$\boldsymbol{B}_j = \begin{bmatrix} \beta_{dj}^0 & \beta_{dj-1}^0 & \beta_{dj-2}^0 & \cdots & \beta_{d(j-1)+1}^0 \\ \beta_{dj}^1 & \beta_{dj-1}^1 & \beta_{dj-2}^1 & \cdots & \beta_{d(j-1)+1}^1 \\ \ddots & \ddots & \ddots & \ddots & \ddots \\ \beta_{dj}^{d-1} & \beta_{dj-1}^{d-1} & \beta_{dj-2}^{d-1} & \cdots & \beta_{d(j-1)+1}^{d-1} \end{bmatrix}. \tag{11}$$

We notice that the structure of the matrix in (10) is the same as in (6), with the latter the scalar case of the former. Therefore, the Hermite problem is the block extension in the matrix sense of the point interpolation problem, and we can take profit of the same kind of linear algebra tools to solve both.

2.2 Some remarks on circulant and ω-circulant matrices

In this section we briefly recall some properties of both circulant and ω-circulant matrices that are needed for our aims. Let us start with the definition of circulant matrices (refer to [7] for more details).

Definition 2.2. *Let* $\boldsymbol{\alpha} = [\alpha_0, \alpha_{-1}, \dots, \alpha_{-n+1}]$ *with* $\alpha_j \in \mathbb{R}$*, and consider* $\alpha_{-j} = \alpha_{n-j}$*. A* circulant matrix $\mathbf{C} = circ(\boldsymbol{\alpha})$*, is defined as satisfying* $(\mathbf{C})_{s,t} = \alpha_{s-t \mod (n)}$*.*

This matrix $\mathbf{C} = \mathrm{circ}(\boldsymbol{\alpha})$ can be represented as

$$\mathbf{C} = \sum_{j=0}^{n-1} \Pi_n^j \alpha_j,$$

where Π_n is the permutation matrix

$$\Pi_n = \begin{bmatrix} 0 & 0 & 0 & \dots & 0 & 1 \\ 1 & 0 & 0 & \dots & 0 & 0 \\ 0 & 1 & 0 & \dots & 0 & 0 \\ 0 & 0 & 1 & \dots & 0 & 0 \\ \ddots & \ddots & \ddots & \ddots & \ddots & \ddots \\ 0 & 0 & 0 & \dots & 1 & 0 \end{bmatrix}.$$

The matrix Π_n can be factorized as:

$$\Pi_n = F_n \Omega_n F_n^*, \tag{12}$$

where F_n is the Fourier matrix defined as

$$F_n = \left[\frac{e^{-2\pi \mathrm{i} jk/n}}{\sqrt{n}} \right]_{j,k=0}^{n-1}, \quad \mathrm{i}^2 = -1,$$

$\cdot^*$ is the conjugate transpose, and

$$\Omega_n = \mathrm{diag}_{s=0,\ldots,n-1}\left(e^{2\pi \mathrm{i} s/n}\right). \tag{13}$$

As a consequence, $\mathbf{C}$ can be diagonalized as $\mathbf{C} = F_n L_n F_n^*$, with

$$L_n = \mathrm{diag}_{s=0,\ldots,n-1}\left(\sum_{j=0}^{n-1} e^{2\pi \mathrm{i} sj/n}\alpha_j\right).$$

Note that the diagonal matrix L_n is defined by the Fourier transform of the first column of $\mathbf{C}$.

Remark 2.3. *In the case where* $\mathbf{C} = \sum_{j=-p}^{q} \Pi_n^j \alpha_j$ *with fixed* $p, q < \lfloor n/2 \rfloor$, *then*

$$\Lambda(\mathbf{C}) = \left\{ f\left(\frac{2\pi j}{n}\right), j = 0, \ldots, n-1 \right\},$$

with $f(\theta) := \sum_{j=-p}^{q} \alpha_j e^{\mathrm{i} j\theta}$ *also called* symbol *of* $\mathbf{C}$.

An extension to the notion of circulant matrices is given by the ω-circulants defined as follows (see, e.g., [5, 3, 20] for more details).

Definition 2.4. *Let* $\boldsymbol{\alpha} = [\alpha_0, \alpha_{-1}, \ldots, \alpha_{-n+1}]$ *with* $\alpha_j \in \mathbb{R}$, *and consider* $\alpha_{-j} = \alpha_{n-j}$. *An* ω-circulant matrix $\mathbf{C}_\omega = \omega - circ(\boldsymbol{\alpha})$, *is defined as satisfying*

$$(\mathbf{C}_\omega)_{s,t} = \begin{cases} \alpha_{s-t}, & \text{if } s > t, \\ \omega\alpha_{s-t}, & \text{if } s < t. \end{cases}$$

The case $\omega = 1$ provides the original circulant matrices.

The matrix $\mathbf{C}_\omega$ can be represented as

$$\mathbf{C}_\omega = \sum_{j=0}^{n-1} \Pi_{n,\omega}^j \alpha_j,$$

where $\Pi_{n,\omega}$ is the matrix

$$\Pi_{n,\omega} = \begin{bmatrix} 0 & 0 & 0 & \ldots & 0 & \omega \\ 1 & 0 & 0 & \ldots & 0 & 0 \\ 0 & 1 & 0 & \ldots & 0 & 0 \\ 0 & 0 & 1 & \ldots & 0 & 0 \\ \ddots & \ddots & \ddots & \ddots & \ddots & \ddots \\ 0 & 0 & 0 & \ldots & 1 & 0 \end{bmatrix}.$$

Let us write $\omega = \rho e^{\mathrm{i}\psi}$ with $\rho > 0$ and consider $\sqrt[n]{\omega} = \sqrt[n]{\rho}\, e^{\mathrm{i}\frac{\psi}{n}}$. Then, thanks to (12), the matrix $\Pi_{n,\omega}$ can be factorized as

$$\Pi_{n,\omega} = \sqrt[n]{\omega} D_\omega \Pi_n D_\omega^{-1} = \sqrt[n]{\omega} D_\omega F_n \Omega_n F_n^* D_\omega^{-1}$$

with $D_\omega = \mathrm{diag}_{s=0,\ldots,n-1}\left(\omega^{-\frac{s}{n}}\right)$ and Ω_n as in (13). Note that this is equivalent to write $\Pi_{n,\omega} = \sqrt[n]{|\omega|} D_\omega F_n \Omega_{n,\omega} F_n^* D_\omega^{-1}$ with

$$\Omega_{n,\omega} = \mathrm{diag}_{s=0,\ldots,n-1}\left(e^{\mathrm{i}(2\pi s+\psi)/n}\right)$$

(compare with (13) for a better understanding of the role of ω).

Let us define $F_{n,\omega} = D_\omega F_n$. As it is expected, for $\omega = 1$ we get $F_{n,1} = F_n$. Then, we get the factorization $\mathbf{C}_\omega = F_{n,\omega} L_{n,\omega} F_{n,\omega}^{-1}$ where

$$L_{n,\omega} = \mathrm{diag}_{s=0,\ldots,n-1}\left(\sum_{j=0}^{n-1} \omega^{j/n} e^{2\pi \mathrm{i} s j/n} \alpha_j\right).$$

Remark 2.5. *In the case where* $\mathbf{C}_\omega = \sum_{j=-p}^{q} \Pi_{n,\omega}^j \alpha_j$ *with fixed* $p, q < \lfloor n/2 \rfloor$, *and* $\omega = e^{\mathrm{i}\psi}$, *then*

$$\Lambda(\mathbf{C}_\omega) = \left\{ f\left(\frac{2\pi j + \psi}{n}\right), j = 0, \ldots, n-1 \right\},$$

with $f(\theta) := \sum_{j=-p}^{q} \alpha_j e^{\mathrm{i}j\theta}$.

We end this section extending both circulants and ω-circulants to the block case.

Definition 2.6. *Let* $\mathcal{A} = [\mathcal{A}_0, \mathcal{A}_{-1}, \ldots, \mathcal{A}_{-n+1}]$ *with* $\mathcal{A}_j \in \mathbb{R}^{m\times m}$, *and consider* $\mathcal{A}_{-j} = \mathcal{A}_{n-j}$. *An* ω-$(m\times m)$-block circulant matrix $\mathcal{C}_\omega = \omega - circ(\mathcal{A})$, *is defined as satisfying*

$$(\mathcal{C}_\omega)_{s,t} = \begin{cases} \mathcal{A}_{s-t}, & \text{if } s > t, \\ \omega \mathcal{A}_{s-t}, & \text{if } s < t. \end{cases}$$

When $\omega = 1$, Definition 2.6 reduces to the definition of $(m \times m)$-block circulant matrices. Also in the block case, ω-circulants can be diagonalized by fast Fourier transforms as follows

$$\begin{aligned} \mathcal{C}_\omega = \sum_{j=0}^{n-1} \Pi_{n,\omega}^j \otimes \mathcal{A}_j &= (D_\omega \otimes I_m)(F_{n,1} \otimes I_m)\mathcal{L}_{n,\omega}(F_{n,1}^* \otimes I_m)(D_\omega^{-1} \otimes I_m) \\ &= (F_{n,\omega} \otimes I_m)\mathcal{L}_{n,\omega}(F_{n,\omega}^{-1} \otimes I_m) \end{aligned}$$

where

$$\mathcal{L}_{n,\omega} = \mathrm{diag}_{s=0,\ldots,n-1}\left(\sum_{j=0}^{n-1} \omega^{j/n} e^{2\pi \mathrm{i} s j/n} \mathcal{A}_j\right), \tag{14}$$

and I_m is the identity of size m.

Remark 2.7. *In the case where* $\mathcal{C}_\omega = \sum_{j=-p}^{q} \Pi_{n,\omega}^j \otimes \mathcal{A}_j$ *with fixed* $p, q < \lfloor n/2 \rfloor$, *and* $\omega = e^{\mathrm{i}\psi}$ *then*

$$\Lambda(\mathcal{C}_\omega) = \left\{ \lambda_k\left(f\left(\frac{2\pi j + \psi}{n}\right)\right),\ k = 1, \ldots, m,\ j = 0, \ldots, n-1 \right\},$$

with $f(\theta) := \sum_{j=-p}^{q} \mathcal{A}_j e^{\mathrm{i}j\theta}$ *an* $m \times m$*-matrix valued function and* $\lambda_k(f(\theta))$, $k = 1, \ldots, m$ *its eigenvalue functions.*

2.3 Our regularizing strategy

Given our problem $M_n\mathbf{P}^0 = \mathbf{V}^0$ in (6), the fact of being M_n a circulant matrix provides us some tools to solve it. Indeed, by Remark 2.3 we have that the spectrum of M_n is given by

$$\Lambda(M_n) = \left\{ b\left(\frac{2\pi j}{n}\right), j = 0, \ldots, n-1 \right\} \tag{15}$$

with the *symbol*

$$b(\theta) := \sum_{k=-p}^{q} \beta_k e^{\mathrm{i}k\theta}$$

independent of n. Thus, the singularity of M_n depends on whether $b(\theta)$ has roots in the grid $\frac{2\pi\mathbb{N}}{n} \cap [0, 2\pi]$.

For odd-symmetric schemes $\boldsymbol{\beta}_n := [\beta_0, \beta_{-1}, \ldots, \beta_{-p}, 0, \ldots, 0, \beta_p, \ldots, \beta_1] \in \mathbb{R}^n$ and so

$$b(\theta) = \sum_{k=-p}^{p} \beta_k e^{\mathrm{i}k\theta} = \beta_0 + 2\sum_{k=1}^{p} \beta_k \cos(k\theta). \tag{16}$$

On the other hand, for even-symmetric schemes $\boldsymbol{\beta}_n := [\beta_0, \beta_{-1}, \ldots, \beta_{-p+1}, 0, \ldots, 0, \beta_p, \ldots, \beta_1] \in \mathbb{R}^n$, then

$$\begin{aligned} b(\theta) &= \sum_{k=-p+1}^{p} \beta_k e^{\mathrm{i}k\theta} = \sum_{k=1}^{p} \beta_k \left(e^{\mathrm{i}(-k+1)\theta} + e^{\mathrm{i}k\theta}\right) = e^{\frac{\mathrm{i}\theta}{2}} \sum_{k=1}^{p} \beta_k \left(e^{\mathrm{i}\left(-k+\frac{1}{2}\right)\theta} + e^{\mathrm{i}\left(k-\frac{1}{2}\right)\theta}\right) \\ &= 2e^{\frac{\mathrm{i}\theta}{2}} \sum_{k=1}^{p} \beta_k \cos\left((2k-1)\tfrac{\theta}{2}\right). \end{aligned} \tag{17}$$

In both cases, the first limit stencil satisfies $b(0) = 1$.

We notice that for odd-symmetric schemes:

$$b(2\pi-\theta) = \beta_0 + 2\sum_{k=1}^{p} \beta_k \cos(k(2\pi-\theta)) = \beta_0 + 2\sum_{k=1}^{p} \beta_k \cos(k\theta) = b(\theta)$$

while for the even-symmetric cases:

$$\begin{aligned} b(2\pi-\theta) &= 2e^{\frac{\mathrm{i}(2\pi-\theta)}{2}} \sum_{k=0}^{p} \beta_k \cos\left((2k-1)\frac{(2\pi-\theta)}{2}\right) = 2e^{\frac{-\mathrm{i}\theta}{2}} \sum_{k=0}^{p} \beta_k \cos\left((2k-1)\tfrac{\theta}{2}\right) \\ &= e^{-\mathrm{i}\theta} b(\theta). \end{aligned}$$

Therefore, it is enough to study the symbol in the interval $[0, \pi]$ to get information about the interval $[0, 2\pi]$. In particular, for every symbol (16) and (17) we have that if $b(\theta) = 0$, then $b(2\pi - \theta) = 0$.

From (17) we get that for even-symmetric schemes $b(\pi) = 0$ independently of the values of n and $\boldsymbol{\beta}$. As π belongs to the grid $\frac{2\pi\mathbb{N}}{n} \cap [0, 2\pi]$ for even n, then by (15) we conclude the following.

Lemma 2.8. *For any even-symmetric subdivision scheme, if the amount of interpolated points n is even, then the interpolation matrix M_n is singular.*

Meanwhile, for the odd-symmetric schemes the symbol could also vanish in the grid $\frac{2\pi\mathbb{N}}{n} \cap [0, 2\pi]$. As an example we can consider the primal family of J-spline schemes [17] for the particular case that generates C^3 subdivision curves:

$$\begin{cases} P_{2i}^{k+1} & = \frac{1}{4}P_{j-1}^k + \frac{1}{2}P_j^k + \frac{1}{4}P_{j+1}^k \\ P_{2j+1}^{k+1} & = \frac{1}{16}P_{j-1}^k + \frac{7}{16}P_j^k + \frac{7}{16}P_{j+1}^k + \frac{1}{16}P_{j+2}^k, \quad k \in \mathbb{N}, j \in \mathbb{Z}, \end{cases} \tag{18}$$

with first limit stencil:

$$\boldsymbol{\beta} = \frac{1}{48}\{1,\ 12,\ 22,\ 12,\ 1\}.$$

In this case, the symbol

$$b(\theta) = \tfrac{11}{24} + \tfrac{1}{2}\cos(\theta) + \tfrac{1}{24}\cos(2\theta) = (\cos(\theta) + 1)\left(\cos(\theta) + \tfrac{1}{5}\right)$$

annihilates at $\theta = \pi$ that belongs to the grid $\frac{2\pi\mathbb{N}}{n} \cap [0, 2\pi]$ when n is an even number.

For the related cases where the matrix is singular, the interpolation problem in (6) may have no solution or infinite many. Those cases are treated in the literature by a fitting model [14] or by a fairness functional [13] while introducing more points as degree of freedom.

In this work we analyze another alternative that consists in solving another regularized problem $M_{n,\omega}\mathbf{P}^0 = \mathbf{V}^0$, exchanging the circulant matrix by a ω-circulant matrix.

For defining our matrix $M_{n,\omega}$ we will use the complex number $\omega = e^{\mathrm{i}\psi}$. Then, by Remark 2.5, the spectrum of our matrix $M_{n,\omega}$ is given by the symbol $b(\theta + \frac{\psi}{n})$. In this way, the eigenvalues of M_n are shifted and, M_n and $M_{n,\omega}$ are both singular if there are at least two roots of $b(\theta)$ in the grid $\frac{2\pi\mathbb{N}}{n} \cap [0, 2\pi]$ with distance $\frac{\psi}{n}$ between them.

When this does not occur, the system of equations $M_{n,\omega}\mathbf{P}^0 = \mathbf{V}^0$ is a perturbation of the initial problem $M_n\mathbf{P}^0 = \mathbf{V}^0$, which has a unique solution when the former does not. The question is then the existence of a complex solution when the original problem is set in the real domain. By choosing ψ small in modulus not only the perturbed system is close to the original one, but the fact to take the real part of the solution is not a bad idea, since the imaginary part is in fact small enough.

In the Hermite interpolation scenario we can find a singular point and tangents interpolation operator even when the point interpolation operator is not singular. Let us consider for example the cubic B-spline scheme, whose first limit stencil is $\{\frac{1}{6}, \frac{4}{6}, \frac{1}{6}\}$ and the second limit stencil is $\{-\frac{1}{2}, 0, \frac{1}{2}\}$. Then, the first one is the matrix:

$$\begin{bmatrix} \frac{4}{6} & \frac{1}{6} & 0 & \dots & 0 & \frac{1}{6} \\ \frac{1}{6} & \frac{4}{6} & \frac{1}{6} & \dots & 0 & 0 \\ \vdots & & & \ddots & & \vdots \\ \frac{1}{6} & 0 & 0 & \dots & \frac{4}{6} & \frac{1}{6} \end{bmatrix}$$

which is not singular, but the second

$$\left[\begin{array}{cc|cc|c|cc|cc} \frac{4}{6} & \frac{1}{6} & 0 & 0 & \multirow{2}{*}{$\dots$} & 0 & 0 & 0 & \frac{1}{6} \\ 0 & \frac{1}{2} & 0 & 0 & & 0 & 0 & 0 & -\frac{1}{2} \\ \hline 0 & \frac{1}{6} & \frac{4}{6} & \frac{1}{6} & \ddots & 0 & 0 & 0 & 0 \\ 0 & -\frac{1}{2} & 0 & \frac{1}{2} & & 0 & 0 & 0 & 0 \\ \hline \multicolumn{2}{c|}{\vdots} & \multicolumn{2}{c|}{\ddots} & \ddots & \multicolumn{2}{c|}{\ddots} & \multicolumn{2}{c}{\vdots} \\ \hline 0 & 0 & 0 & 0 & \dots & 0 & \frac{1}{6} & \frac{4}{6} & \frac{1}{6} \\ 0 & 0 & 0 & 0 & & 0 & -\frac{1}{2} & 0 & \frac{1}{2} \end{array}\right]$$

is singular with kernel of dimension 1.

Indeed, the following holds for the particular case of point and tangent interpolation with odd-symmetric schemes.

Lemma 2.9. *For an odd-symmetric subdivision scheme and $d = 2$, it holds that the matrix $\mathbf{M}_n$ is singular.*

Proof. For odd-symmetric schemes we have from (14) and (11) that the $(1,1)$-block of $\mathcal{L}_n$ is:

$$\begin{aligned}(\mathcal{L}_n)_{1,1} &= \sum_{j=0}^{\lceil \frac{p}{2} \rceil} \begin{bmatrix} \beta^0_{-2j} & \beta^0_{-2j-1} \\ \beta^1_{-2j} & \beta^1_{-2j-1} \end{bmatrix} + \sum_{j=1}^{\lceil \frac{p}{2} \rceil} \begin{bmatrix} \beta^0_{2j} & \beta^0_{2j-1} \\ \beta^1_{2j} & \beta^1_{2j-1} \end{bmatrix} \\ &= \begin{bmatrix} \beta^0_0 & \beta^0_1 \\ \beta^1_0 & -\beta^1_1 \end{bmatrix} + \sum_{j=1}^{\lceil \frac{p}{2} \rceil} \begin{bmatrix} \beta^0_{2j} & \beta^0_{2j-1} \\ -\beta^1_{2j} & -\beta^1_{2j+1} \end{bmatrix} + \sum_{j=1}^{\lceil \frac{p}{2} \rceil} \begin{bmatrix} \beta^0_{2j} & \beta^0_{2j-1} \\ \beta^1_{2j} & \beta^1_{2j-1} \end{bmatrix} \\ &= \begin{bmatrix} \beta^0_0 + 2\sum_{j=1}^{\lceil \frac{p}{2} \rceil} \beta^0_{2j} & 2\sum_{j=1}^{\lceil \frac{p}{2} \rceil} \beta^0_{2j-1} \\ 0 & 0 \end{bmatrix}, \end{aligned} \tag{19}$$

given that $\beta^1_0 = 0$ in (7). As there is a null row in (19), it follows that the block $(\mathcal{L}_n)_{1,1}$ is singular and then also the matrices $\mathcal{L}_n$ and $\mathbf{M}_n$, because of (14). □

If we consider the corresponding ω-circulant matrix $M_{n,\omega}$ we get that the block in (19) becomes:

$$\begin{aligned}(\mathcal{L}_{n,\omega})_{1,1} &= \sum_{j=0}^{\lceil \frac{p}{2} \rceil} \boldsymbol{B}_j \; \omega^{j/n} + \sum_{j=1}^{\lceil \frac{p}{2} \rceil} \boldsymbol{B}_{-j} \; \omega^{(n-j)/n} \\ &= \begin{bmatrix} \beta^0_0 & \beta^0_1 \\ \beta^1_0 & -\beta^1_1 \end{bmatrix} + \sum_{j=1}^{\lceil \frac{p}{2} \rceil} \begin{bmatrix} \beta^0_{2j} & \beta^0_{2j-1} \\ \beta^1_{2j} & \beta^1_{2j-1} \end{bmatrix} \omega^{j/n} + \sum_{j=1}^{\lceil \frac{p}{2} \rceil} \begin{bmatrix} \beta^0_{2j} & \beta^0_{2j+1} \\ -\beta^1_{2j} & -\beta^1_{2j+1} \end{bmatrix} \omega^{(n-j)/n} \\ &= \begin{bmatrix} \beta^0_0 + \sum_{j=1}^{\lceil \frac{p}{2} \rceil} \beta^0_{2j} \left(\omega^{j/n} + \omega^{(n-j)/n}\right) & \beta^0_1 \left(1 + \omega^{(n-1)/n}\right) + \sum_{j=2}^{\lceil \frac{p}{2} \rceil} \beta^0_{2j-1} \left(\omega^{j/n} + \omega^{(n-j)/n}\right) \\ \sum_{j=1}^{\lceil \frac{p}{2} \rceil} \beta^1_{2j} \left(\omega^{j/n} - \omega^{(n-j)/n}\right) & \beta^1_1 \left(\omega^{1/n} - 1\right) + \sum_{j=2}^{\lceil \frac{p}{2} \rceil} \beta^1_{2j-1} \left(\omega^{j/n} - \omega^{(n-j)/n}\right) \end{bmatrix}. \end{aligned}$$

Then, the singularity of M_n does not imply the singularity of $M_{n,\omega}$ and the system $M_{n,\omega}\mathbf{P}^0 = \mathbf{U}^{(d)}$ can be solved instead of (10). In this general case, the symbol does not follow the same structure as in (16) and (17), but a more involved one.

Remark 2.10. *We mention that in [15] the point and tangent interpolation problem, for the particular case of cubic B-spline curves, is solved but just considering the case of unitary tangents V^1_j, $j = 0, \ldots, n-1$. Their proposal is a non-linear iterative method, without theoretical proved convergence.*

3 Numerical tests

In this section we analyze the quality of the solution obtained by adopting the ω-circulant regularization when we are in presence of a singular interpolation operator. In all examples we test with the J-spline family [17].

Let us denote by $\hat{\mathbf{P}}^0$ and $\hat{\mathbf{P}}^0_\omega$, the control point vectors obtained as $M_n^\dagger \mathbf{U}^{(d)}$ and $M_{n,\omega}^\dagger \mathbf{U}^{(d)}$, respectively. We use the pseudo-inverse $M_{n,\omega}^\dagger$ defined as

$$M_{n,\omega}^\dagger = (F_{n,\omega} \otimes I_m)\mathcal{L}_{n,\omega}^\dagger (F_{n,\omega}^{-1} \otimes I_m), \quad \text{with } (\mathcal{L}_{n,\omega}^\dagger)_k = \begin{cases} \frac{1}{(\mathcal{L}_{n,\omega})_k} & , \text{ if } (\mathcal{L}_{n,\omega})_k \neq 0, \\ 0 & , \text{ if } (\mathcal{L}_{n,\omega})_k = 0, \end{cases}$$

where $(\mathcal{L}_{n,\omega})_k$ is the k-th element in the diagonal matrix reported in (14). For $\omega = 1$ we readily obtain $M_n^\dagger$.

From the control point vectors $\hat{\mathbf{P}}^0$ and $\hat{\mathbf{P}}^0_\omega$ we generate the associated subdivision curves and we make a comparison between them. In order to evaluate their quality, proper fairness measures can be used [1, 21]. In our tests we always compare in 2-norm, denoted by $\|\cdot\|$.

In every figure we draw the curve obtained with the least square solution $\hat{\mathbf{P}}^0$ with dotted blue lines and the one obtained with the regularized solution $\hat{\mathbf{P}}^0_\omega$ with solid red lines.

If a non singular matrix is used, then the solution by using the ω-circulant matrix still interpolates the given points. Indeed, in Fig. 1 we see only one line because both solutions, $\hat{\mathbf{P}}^0$ and $\hat{\mathbf{P}}^0_\omega$ match. Here we choose $\omega = e^{5\cdot 10^{-3}\mathrm{i}}$, but values close to this still work. Therefore, the perturbation with the parameter ω does not affect the quality of the interpolating solution.

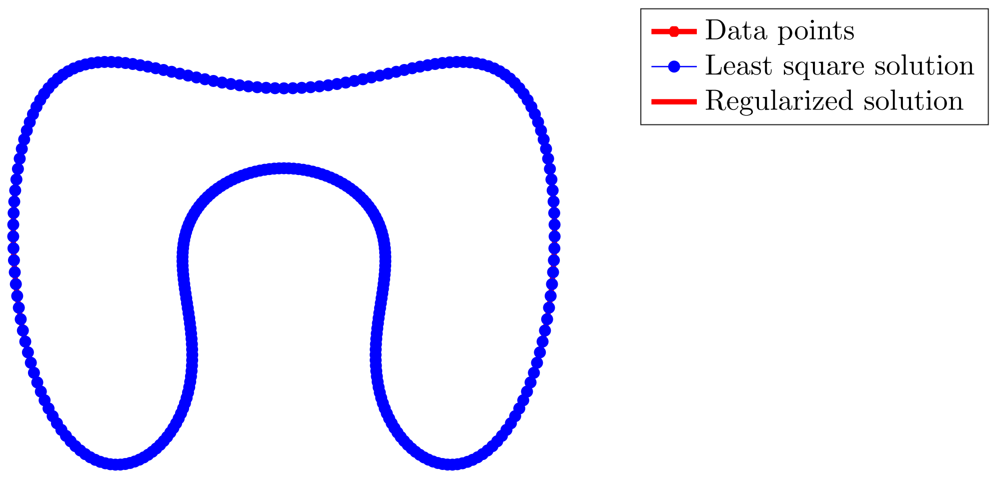

Figure 1: Point interpolation with a quintic B-spline curve (that belongs to the J-spline family). Blue dotted line: least square solution. Red solid line: regularized solution.

If we consider a primal scheme with odd-symmetric mask like in (18), for which the interpolation operator is singular, we obtain a least square solution that does not interpolate the data points. The spectrum of M_n is perturbed with the consideration of a regularized solution as shown in Fig. 3 and the condition number improves by the shifting of the null value in the spectrum, but the solution does not improve the approximation as Fig. 2 shows for the parameter $\omega = e^{5\cdot 10^{-2}\mathrm{i}}$. The residual norms are

$$\|\mathbf{U}^{(d)} - M_n \hat{\mathbf{P}}^0\| = 0.0622 \quad \text{and} \quad \|\mathbf{U}^{(d)} - M_{n,\omega} \hat{\mathbf{P}}^0\| = 0.0683.$$

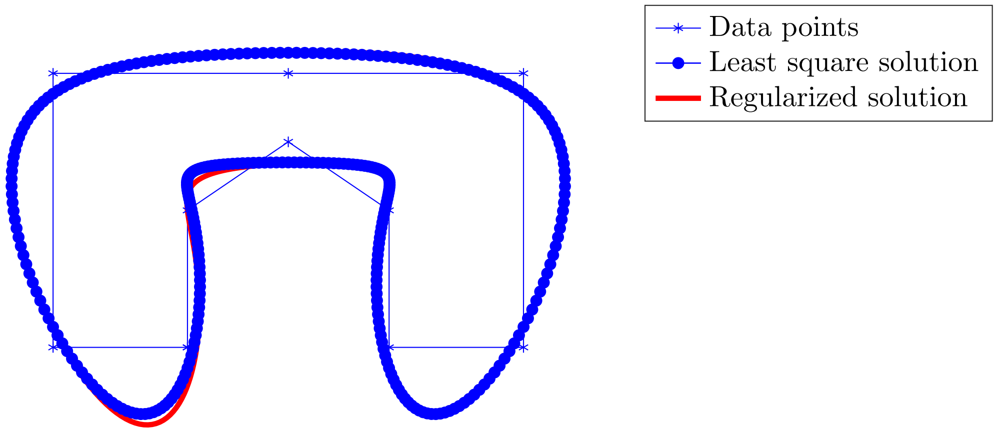

Figure 2: Point interpolation with a J-spline curve (18) with singular interpolation operator (that belongs to the J-spline family). Blue dotted line: least square solution. Red solid line: regularized solution.

In the block case for point and tangent interpolation we have a similar situation. Although the spectrum of $M_{n,\omega}$ is perturbed with respect to M_n and does not have a null value like the spectrum of the latter (see Fig. 5), the quality of the solution does not improve (see Fig. 4 where $\omega = e^{5\cdot 10^{-1}\mathrm{i}}$). It is worth noticing that the points are interpolated, but the tangent interpolation is less accurate. In this case the residual norms are

$$\|\mathbf{U}^{(d)} - M_n\hat{\mathbf{P}}^0\| = 2.4953e - 16 \quad \text{and} \quad \|\mathbf{U}^{(d)} - M_{n,\omega}\hat{\mathbf{P}}^0\| = 0.01183.$$

Nevertheless, if we consider as a test case an already known solution, i.e., if we know already the solution $\mathbf{P}^0$ and we generate $\mathbf{U} = M_n\mathbf{P}^0$, then we can obtain for a suitable parameter ω a solution that interpolates the points just as the least square solution does (refer to Fig. 6 where $\omega = e^{5\cdot 10^{-3}\mathrm{i}}$), even though the spectra of M_n and $M_{n,\omega}$ are different (see Fig. 7).

4 Conclusions

In this work we compared the solution obtained with the least square solution and the regularization with an ω-circulant for the point interpolation problem. As an extension we studied also the Hermite interpolation for point and tangent vectors. Specifically, since in some cases the interpolation problem brings to a singular matrix M_n, the situation is tackled by the perturbation of the spectrum of M_n switching to its ω-circulant counterpart $M_{n,\omega}$.

However, the proposed ω-regularization approach is not enough to solve the problem. Although the new matrix $M_{n,\omega}$ is better conditioned when the original M_n is singular, it does not always represent exactly the interpolation condition, which affects the quality of the approximation. Nonetheless, for some cases with known solution, the linear system associated to $M_{n,\omega}$ provides a numerical solution that interpolates the data points. Since this positive aspect does not occur in several cases, it remains the open problem of a further step of correction.

Another open problem which remains is to establish, both in the scalar and in the block settings, whether the solution $\mathrm{Sol}(e^{\mathrm{i}\psi})$ has an asymptotic expansion with respect to the small

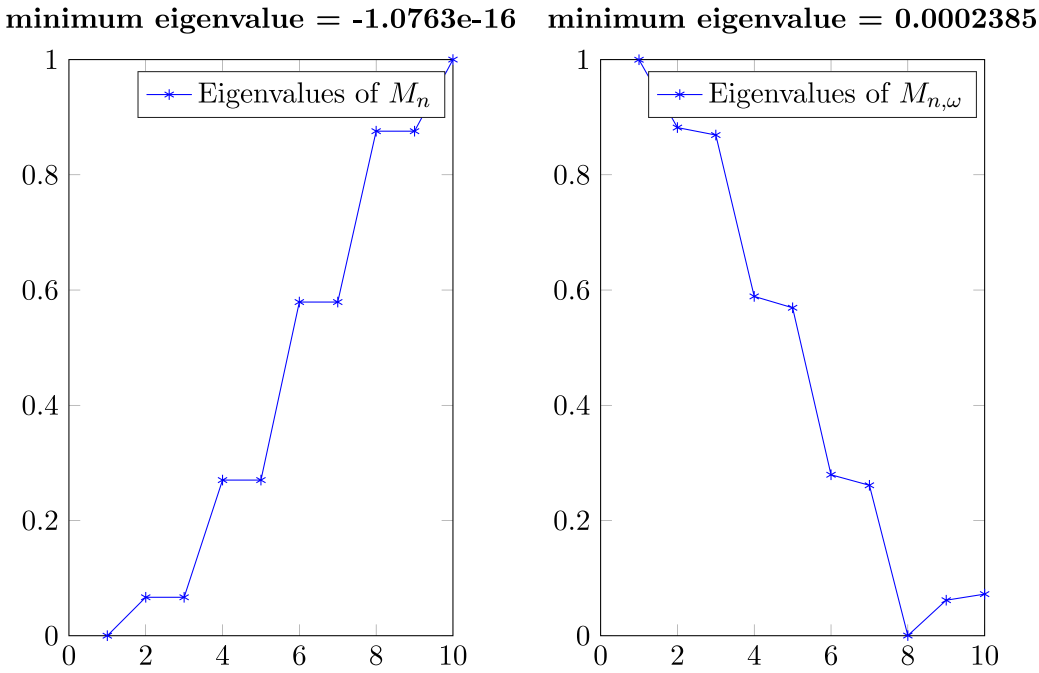

Figure 3: Eigenvalues of M_n and $M_{n,\omega}$.

parameter ψ of the form

$$\mathrm{Sol}(e^{i\psi}) = \mathrm{Sol} + c_1\psi + c_2\psi^2 + c_3\psi^3 + \cdots .$$

If the latter fact would be true, then simple and cheap extrapolation procedures could be applied for computing much precise solutions. Preliminary numerical results are available and encouraging, but the picture is not clear. We believe that this study would deserve more attention in future investigations.

Finally, another possible strategy to avoid singular matrices in the interpolation problem that we plan to investigate is to suppose the parameterization $V_j^0 = c(j+\sigma)$ or $V_j^k = c^{(k)}(dj+\sigma)$ for the respective point interpolation and Hermite interpolation cases in (4) and (9), motivated by Plonka's work [16] for Hermite interpolation with B-spline.

References

[1] G. Albrecht, *Invariante Gütekriterien im Kurvendesign - Einige neuere Entwicklungen*, Effiziente Methoden der geometrischen Modellierung und der wissenschaftlichen Visualisierung / Dagstuhl-Seminar 1997 (H. Hagen et al., ed.), Springer, 1999, pp. 134–148.

[2] L. E. Andersson and N. F. Stewart, *Introduction to the mathematics of subdivision surfaces*, SIAM, 2010.

[3] D. Bini, *Parallel solutions of certain Toeplitz linear systems*, SIAM Journal on Computing **13** (1984), no. 2, 268–276.

[4] C. Chui and J. de Villiers, *Wavelet subdivision methods: Gems for rendering curves and surfaces*, CRC Press, 2010.

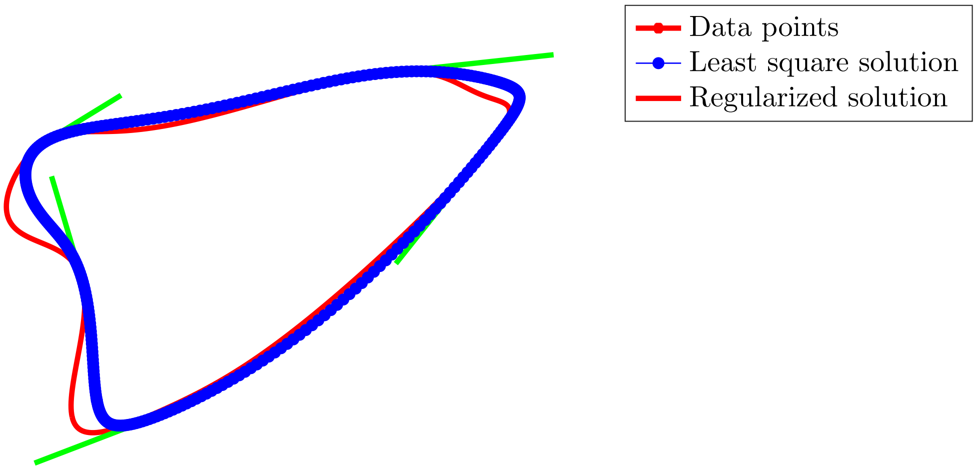

Figure 4: Point and tangent vectors interpolation with a quintic B-spline curve (that belongs to the J-spline family). Blue dotted line: least square solution. Red solid line: regularized solution.

[5] R. E. Cline, R. J. Plemmons, and G. Worm, *Generalized inverses of certain Toeplitz matrices*, Linear Algebra and its Applications **8** (1974), no. 1, 25–33.

[6] I. Daubechies, I. Guskov, and W. Sweldens, *Commutation for irregular subdivision*, Constructive Approximation **17** (2001), 479–514.

[7] P. Davis, *Circulant matrices*, J. Wiley and Sons, 1979.

[8] N. Dyn, *Linear and Nonlinear Subdivision Schemes in Geometric Modeling*, School of Mathematical Sciences, Tel Aviv University, 2008.

[9] N. Dyn, M. S. Floater, and K. Hormann, *A C^2 four-point subdivision scheme with fourth order accuracy and its extensions*, Mathematical methods for curves and surfaces: TROMS 2004, Modern methods in Mathematics, Nashboro Press, 2005, pp. 145–156.

[10] N. Dyn, J. A. Gregory, and D. Levin, *Analysis of uniform binary subdivision schemes for curve design*, Constructive Approximation **7** (1991), no. 1, 127–147.

[11] N. Dyn and D. Levin, *Subdivision schemes in geometric modelling*, Acta Numerica **11** (2002), 73–144.

[12] N. Dyn, D. Levin, and J. A. Gregory, *A 4-point interpolatory subdivision scheme for curve design*, Computer Aided Geometric Design **4** (1987), 257–268.

[13] M. A. Halstead, M. Kass, and T. DeRose, *Efficient, fair interpolation using Catmull-Clark surfaces*, SIGGRAPH'93, 1993, pp. 35–44.

[14] H. Hoppe, T. DeRose, T. Duchamp, M. Halstead, H. Jin, J. McDonald, J. Schweitzer, and W. Stuetzle, *Piecewise smooth surface reconstruction*, SIGGRAPH 94, 1994, pp. 295–302.

[15] S. Okaniwa, A. Nasri, H. Lin, A. Abbas, Y. Kineri, and T. Maekawa, *Uniform B-spline curve interpolation with prescribed tangent and curvature vectors*, IEEE Transactions on Visualization and Computer Graphics **18** (2012), no. 9, 1474–1487.

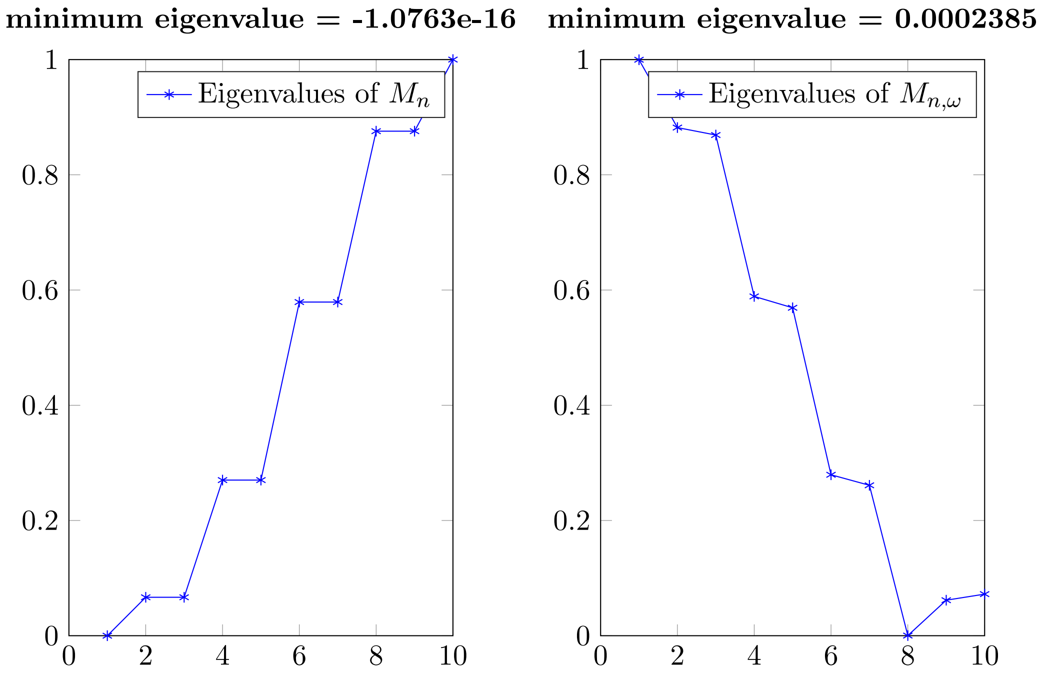

Figure 5: Eigenvalues of M_n and $M_{n,\omega}$.

[16] G. Plonka, *An efficient algorithm for periodic hermite spline interpolation with shifted nodes*, Numerical Algorithms **5** (1993), 51–62.

[17] J. Rossignac and S. Schaefer, *J-splines*, Computer Aided Design **40** (2008), no. 10–11, 1024–1032.

[18] M. Sabin, *Analysis and Design of Univariate Subdivision Schemes*, Springer, 2010.

[19] S. Schaefer and J. Warren, *Exact evaluation of limits and tangents for non-polynomial subdivision schemes*, Computer Aided Geometric Design **25** (2008), no. 8, 607–620.

[20] S. Serra-Capizzano, *A Korovkin-type theory for finite Toeplitz operators via matrix algebras*, Numerische Mathematik **82** (1999), 117–142.

[21] R. C. Veltkamp and W. Wesselink, *Modeling 3D curves of minimal energy*, Computer Graphics Forum **14** (1995), 97–110.

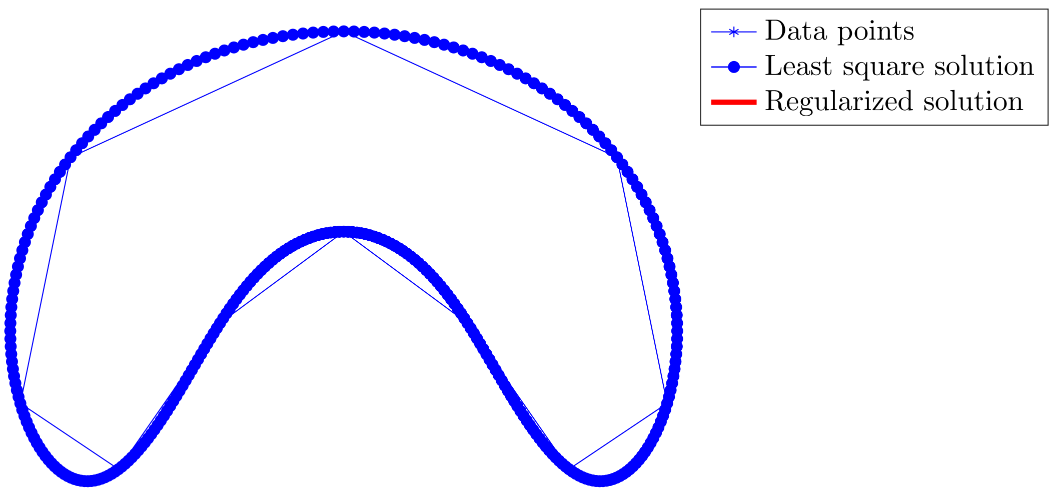

Figure 6: Point interpolation with a J-spline curve (18) with singular interpolation operator for a known solution. Blue dotted line: least square solution. Red solid line: regularized solution.

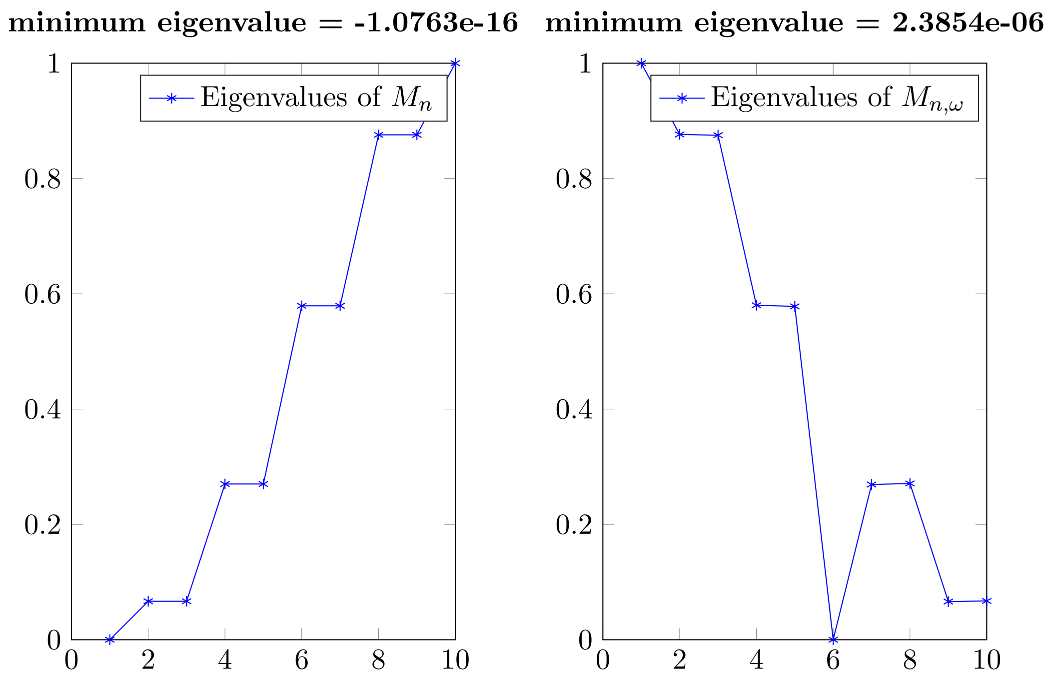

Figure 7: Eigenvalues of M_n and $M_{n,\omega}$.